

# Dynamic thermal relaxation in copper films

L. B. Wang,<sup>1,\*</sup> D. S. Golubev,<sup>1</sup> Y. M. Galperin,<sup>2,3</sup> and J. P. Pekola<sup>1</sup>

<sup>1</sup>*QTF Centre of Excellence, Department of Applied Physics, Aalto University, FI-00076 Aalto, Finland*

<sup>2</sup>*Department of Physics, University of Oslo, PO Box 1048, Blindern, 0316 Oslo, Norway*

<sup>3</sup>*A. F. Ioffe Physical-Technical Institute, Russian Academy of Science, St. Petersburg 194021, Russia*  
(Dated: April 15, 2022)

We present an experimental study of dynamic thermal relaxation in copper films at sub-kelvin temperatures. We detect fast microsecond scale changes of the electron temperature of the film in response to Joule heating with a proximity Josephson junction thermometer. We find that temperature relaxation is characterized by two time constants, one of them is consistent with the conventional theory, while the second one is about one order of magnitude longer. Annealing of the film changes the parameters of the relaxation process. We explain these observations by the existence of an additional thermal reservoir coupled to the film electrons. Fitting the experimental results to this model, we determine the specific heat of this reservoir and its thermal coupling to electrons. We argue that our findings may be explained by the complicated morphology of the copper films, in which electron-phonon coupling strength in grains with different orientations varies.

Proper understanding of thermal transport in mesoscopic devices is essential for the development of low temperature detectors [1]. Heat transport experiments at these temperatures are usually carried out in steady-state conditions, in which temperatures do not depend on time. For example, transport through a single heat-conducting channel has been studied in steady-state [2–6]. Here we focus on thermal relaxation process in a copper (Cu) film and study the time dependence of the electron temperature after an applied heating is turned off, as shown in Fig. 1. Such experiments are particularly important, for example, for the development of Transition Edge Sensors [7–10], normal-metal hot-electron detectors [11–13] and other types of microcalorimeters. Indeed, thermal relaxation determines the time needed for such a device to recover after a detection event.

Typically, thermal relaxation in a normal metal film at low temperatures is determined by electron-phonon coupling, and the relaxation time  $\tau_{e-ph}$  is given by the ratio  $\gamma/5\Sigma T^3$  [14]. Here  $\gamma$  is the Sommerfeld constant, which determines the heat capacity of electrons,  $C_e = \gamma VT$ , with  $V$  the volume of the film, and  $\Sigma$  the characteristic electron-phonon coupling constant defining the heat flux  $P_{e-ph}$  between electron and phonon sub-systems having the temperatures  $T_e$  and  $T_{ph}$ ,  $P_{e-ph} = \Sigma V(T_e^5 - T_{ph}^5)$ . For Cu, these two parameters take the values  $\gamma = 98 \text{ JK}^{-2}\text{m}^{-3}$  [15] and  $\Sigma = 2 \text{ nWK}^{-5}\mu\text{m}^{-3}$  [14, 16], which results in a relaxation time  $\tau_{e-ph} \sim 10 \mu\text{s}$  at 100 mK. In the past, the lack of sufficiently fast and sensitive thermometers hindered the investigation of the dynamic thermal relaxation in the experiments with direct heating of electrons by bias current.

Recently, several types of fast thermometers have been developed, which made it possible to study the dynamic thermal relaxation in metallic systems [17–21]. In our experiment, we have used the fast proximity Josephson junction (JJ) thermometer. Thanks to its high sensitivity and good time resolution, we are able to demonstrate

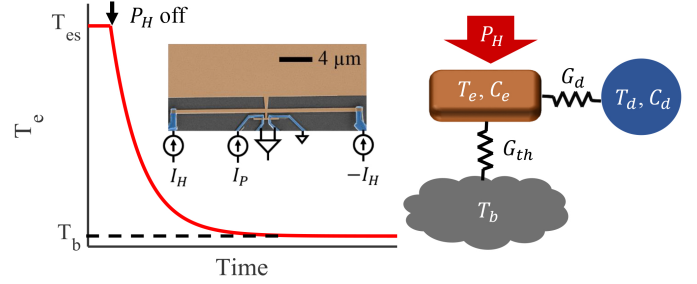


FIG. 1. Left panel: Time dependence of the electron temperature  $T_e$  in response to the external heating power  $P_H$ . After  $P_H$  is switched off, the electron temperature relaxes to the bath temperature  $T_b$ . Inset: False-color SEM image of a typical sample with the measurement circuits. (Cu is shown in brown, Al in blue). Right panel: Thermal model of a heated Cu film on a dielectric substrate. Film electrons are thermally coupled to the bath ( $T_b$ ) and to an additional thermal reservoir ( $T_d, C_d$ ) by thermal conductances  $G_{th}$  and  $G_d$ .

that the relaxation of electron temperature in Cu films is characterized by several time constants. We have observed the same effects in silver (Ag) films [22]. Our results suggest that this phenomenon is caused by the combined effect of strong anisotropy of electron-phonon scattering rate in bulk Cu and Ag [23–27] and of the complex texture of thin films, which contain grains with different orientations relative to the substrate [28, 29].

One of our devices is shown as a false-color SEM image in the inset of Fig. 1. Cu films of varying thicknesses are evaporated on  $\text{SiO}_2/\text{Si}$  substrate with the electron-beam evaporation technique. Superconducting aluminum (Al) is used for the galvanic connection to the Cu films. The large pad on top (partly shown) constitutes the main volume of the film to be studied. Long horizontal Cu wire in the middle is used as a heater, it is biased with currents of opposite polarities  $\pm I_H$ . The short wire at the bottom, which contacts two aluminum leads at both ends,

behaves as a proximity JJ. It is used as a fast thermometer to monitor electron temperature in the Cu film. In the explored temperature range its resolution was around 0.1 mK for a probing pulse of 2  $\mu\text{s}$  duration [22]. Details of the measurement technique have been reported earlier [19].

In the inset of Fig. 2 (a) we show the time dependence of the electron temperature for the two heating current pulses with inverse polarities. Each current pulse has a width of 500  $\mu\text{s}$ , and they were applied during the time intervals  $-3.5$  to  $-3$  ms and  $-0.5$  to 0 ms. The thickness of the Cu film was 300 nm. Before the heating pulse was applied, i.e. for  $-4 < t < -3.5$  ms, the electrons were in thermal equilibrium having the bath temperature  $T_b$ . After the heating was turned on, the electron temperature began to rise and finally reached the steady-state value  $T_{es}$ . Identical responses to the two heating pulses confirm the accuracy of our measurement technique. The steady-state temperature rise  $\Delta T_{es} = T_{es} - T_b$  is consistent with the previous DC measurements [30]. It decreases at high  $T_b$  due to the increase of the thermal conductance between the electrons in the film and the environment.

In order to investigate the dynamic thermal relaxation,

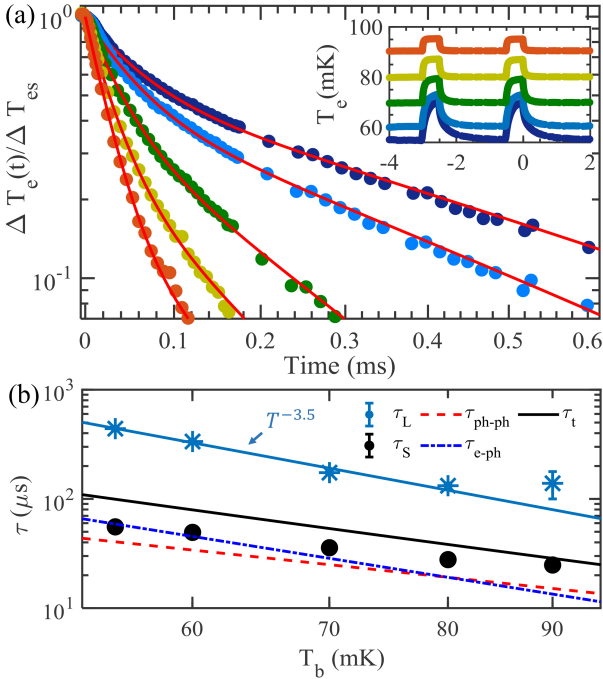


FIG. 2. Thermal relaxation in a 300 nm thick Cu film. (a) Time dependence of the normalized electron temperature  $\Delta T_e(t)/\Delta T_{es}$ . Bath temperatures are  $T_b = 55, 60, 70, 80, 90$  mK from right to left. Red lines are fits with Eq. (1). Inset: electron temperature versus time, the values of  $T_b$  are the same as in the main plot. (b) Temperature dependence of the two time constants  $\tau_L$  and  $\tau_S$ .  $\tau_{e-ph}$  (dash-dotted),  $\tau_{ph-ph}$  (dashed) and  $\tau_t$  (solid black) are the theory predicted time constants given by Eqs. (4). The solid-blue line shows a simple power law fit of the dependence  $\tau_L(T)$ .

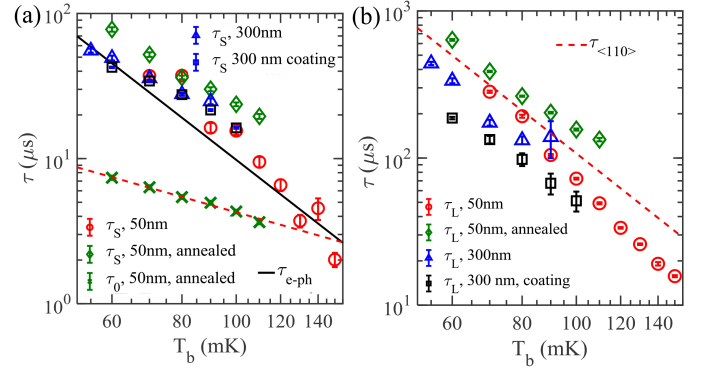


FIG. 3. Temperature dependence of thermal relaxation times for all studied samples. (a) Short time constant  $\tau_S$  (for the annealed 50 nm film we show both  $\tau_S$  and the shortest relaxation time  $\tau_0$ ). Black-solid line shows the calculated electron-phonon time  $\tau_{e-ph}$  (4); red-dashed line is the linear fit of  $\tau_0$  of the annealed 50 nm film. (b) Longer relaxation time  $\tau_L$  versus temperature. Red-dashed line shows the electron-phonon relaxation time of electrons moving in  $\langle 110 \rangle$  direction, which has been measured in bulk Cu,  $\tau_{\langle 110 \rangle} = 10^{-7} \times (T/1\text{K})^{-3}$  s [23].

we have recorded the time dependence of the electron temperature after the heating current is turned off. Figure 2 (a) shows the normalized  $\Delta T_e(t)$  as a function of the time  $t$ . We have found, contrary to our expectation, that the dependence  $\Delta T_e(t)$  could not be fitted with an exponentially decaying function. However, we could very well fit the data with two exponents,

$$\Delta T_e(t)/\Delta T_{es} = ae^{-\frac{t}{\tau_L}} + (1-a)e^{-\frac{t}{\tau_S}}, \quad (1)$$

where  $a$  is a constant pre-factor, and  $\tau_S$  and  $\tau_L$  are, respectively, the short and the long relaxation times. Red lines in Fig. 2 (a) show the corresponding fits. The times  $\tau_S$  and  $\tau_L$  for different temperatures are shown in Fig. 2 (b). At low temperatures the time constant  $\tau_L$  is about one order of magnitude longer than  $\tau_S$ , and at high temperatures  $\tau_L$  and  $\tau_S$  differ even more. As a result, at high temperatures  $\tau_S$  cannot be resolved and the relaxation process takes a single exponential form with a time constant  $\tau_L$ . This explains previous observations of very long relaxation times in Cu and AuPd films [13, 17]. Due to the high sensitivity of our JJ thermometer at low temperatures, we can now clearly distinguish the two time constants. Performing simple power law fits, we find that the relaxation times scale with temperature as  $\tau_L \propto T^{-3.5}$  and  $\tau_S \propto T^{-3}$ . We have also verified that the effect of the heating pulse amplitude on thermal relaxation is negligible for temperature increments within the range 6 mK  $< \Delta T_{es} < 18$  mK [22].

We have repeated the measurements with several films in order to test the dependence of the relaxation times on the film thickness, which has been observed earlier [31]. Such dependence would suggest that multiple relaxation times may be caused by impurities or defects on

the surface of the film. To verify this, we have fabricated a sample with a film thickness of 50 nm, in which the surface to volume ratio is increased by a factor of 6, and a sample with 300 nm Cu film coated with a 5 nm thin layer of Al right after evaporation. The volumes of these two films were the same as the volume of the original 300 nm film, which was  $120 \mu\text{m}^3$ . We have found that both films show two time constants, which are quite close to the ones of the 300 nm film without surface coating, as shown in Fig. 3 (a). Finally, we have measured an annealed 50 nm thin Cu film in order to test the effect of the grain size and grain interface on thermal relaxation. SEM pictures of the sample show significant growth of the grain size after annealing [22]. Thermal relaxation of the annealed film has changed significantly, and we needed three exponents with different relaxation times in order to fit the dependence  $\Delta T_e(t)$  with sufficient accuracy. These time constants are also shown in Fig. 3. The longest and the middle of them are of the same order of magnitude as the times  $\tau_L$  and  $\tau_S$  measured in other samples. The shortest time constant of the annealed film  $\tau_0$  is about 6 - 10 times smaller than  $\tau_S$ , and has a linear dependence on temperature.

Summarizing these observations, we conclude that the appearance of an additional long relaxation time  $\tau_L$  cannot be explained by surface effects. One may alternatively relate it to magnetic impurities in the bulk of the films. However, previous experiment [31] has ruled out such possibility for Cu films. It was found in Ref. [31] that Cu films with very low concentration of magnetic impurities still exhibited long relaxation time. In contrast, less pure silver (Ag) film had only shown short relaxation time  $\tau_S$ , and its value was in good agreement with the predictions of free electron model. We argue below that the origin of the multi-scale thermal relaxation should be rather explained by the morphology of the films.

In order to analyze the two scale relaxation of the electron temperature on the quantitative level, we propose a phenomenological model, in which the electrons in the Cu film are coupled to phonons and to an additional thermal reservoir, as shown in Fig. 1. In this model, the time evolution of temperatures follows the equations

$$\begin{aligned} C_e \frac{dT_e}{dt} &= -\Sigma V(T_e^5 - T_{ph}^5) - \Sigma_d(T_e^\alpha - T_d^\alpha) + P_H(t), \\ C_{ph} \frac{dT_{ph}}{dt} &= \Sigma V(T_e^5 - T_{ph}^5) - \kappa A(T_{ph}^4 - T_b^4), \\ C_d \frac{dT_d}{dt} &= \Sigma_d(T_e^\alpha - T_d^\alpha). \end{aligned} \quad (2)$$

Here  $C_d$  is the heat capacity of the thermal reservoir,  $T_d$  is its temperature,  $\Sigma_d$  is the constant characterizing the coupling between electrons and the reservoir,  $A$  is the contact area between the film and the dielectric substrate,  $\kappa$  is the constant characterizing thermal boundary conductance between the phonons in the film and in the

substrate,  $C_{ph}$  is the heat capacity of the phonons in the film,  $C_e = \gamma V T_e$  is the heat capacity of electrons,  $\alpha$  is an unknown exponent, and  $P_H(t)$  is the heating power. The phonon heat capacity is usually very small, and one can put  $C_{ph} = 0$ . Adopting this approximation and considering linearized versions of Eqs. (2), which are valid at sufficiently small  $P_H$ , we obtain  $\Delta T_e(t)$  after an abrupt removal of the heating in the form of Eq. (1) with the relaxation times and the pre-factor  $a$  having the form

$$\begin{aligned} \frac{1}{\tau_{L,S}} &= \frac{1}{2} \left[ \frac{1}{\tau_d} + \frac{1}{\tau_t} \right] \mp \sqrt{\frac{1}{4} \left[ \frac{1}{\tau_t} - \frac{1}{\tau_d} \right]^2 + \frac{C_d}{C_e + C_d} \frac{1}{\tau_t \tau_d}}, \\ a &= \frac{\tau_d^{-1} - \tau_L^{-1}}{\tau_S^{-1} - \tau_L^{-1}} \frac{\tau_d}{\tau_S}. \end{aligned} \quad (3)$$

The time  $\tau_d$ , appearing above, characterizes the relaxation between electrons and the additional thermal reservoir,  $\tau_d^{-1} = (C_d^{-1} + C_e^{-1})G_d$ , and  $\tau_t$  is the relaxation time of the electron temperature in the absence of the reservoir. It is given by the sum of two contributions,

$$\begin{aligned} \tau_t &= \tau_{e-ph} + \tau_{ph-ph}, \\ \tau_{e-ph} &= \frac{C_e}{G_{e-ph}}, \quad \tau_{ph-ph} = \frac{C_e}{G_{ph-ph}}. \end{aligned} \quad (4)$$

In the above expressions,  $G_d = \alpha \Sigma_d T^{\alpha-1}$  is the thermal conductance between electrons and the reservoir,  $G_{e-ph} = 5 \Sigma V T^4$  is the thermal conductance between electrons and phonons, and  $G_{ph-ph} = 4 \kappa A T^4$  is the thermal conductance between the phonons in the film and in the substrate. In Fig. 2 (b) we plot the times  $\tau_{e-ph}$ ,  $\tau_{ph-ph}$  and  $\tau_t$ , given by Eqs. (4), with the constants  $\Sigma = 2 \text{ nWK}^{-5} \mu\text{m}^{-3}$  and  $\kappa = 60 \text{ pWK}^{-4} \mu\text{m}^{-2}$  measured in an independent steady-state experiment [30]. We observe rather good agreement between the measured values of  $\tau_S$  and the calculated times  $\tau_t$ .

Next, we invert the Eqs. (3,4) and express the heat capacity of the thermal reservoir,  $C_d$ , and the thermal conductance,  $G_d$ , in terms of measured parameters,

$$C_d = [(\tau_L - \tau_S)^2 / \tau_L \tau_S] a (1 - a) \gamma V T, \quad (5)$$

$$G_d = [C_d C_e / (C_d + C_e)] (\tau_L^{-1} + \tau_S^{-1} - \tau_t^{-1}). \quad (6)$$

These values are plotted for three different films in Figs. 4 (a) and (b). The heat capacity  $C_d$  does not exhibit clear temperature dependence in the explored temperature range. Its value is rather high and comparable to the heat capacity of electrons  $C_e$ . It is unlikely that low concentration impurities would result in such a high value. We believe that the most natural reason for that would be the existence of a significant number of grains in the film, which remain electrically decoupled from it. Such grains would form an additional thermal reservoir, which we have postulated in our model. In Fig. 4 (b) we show the temperature dependence of the thermal conductance  $G_d$ . For the two 300 nm films  $G_d$  is almost constant,

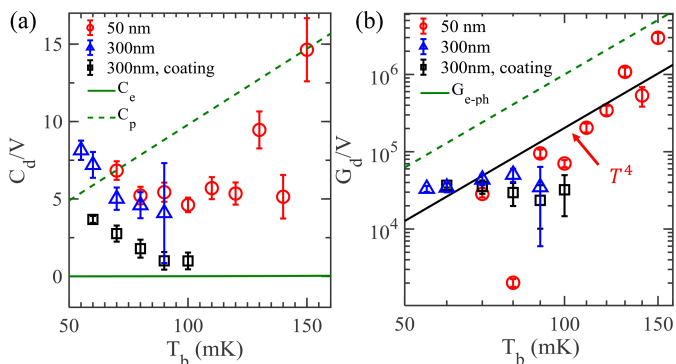


FIG. 4. (a) Temperature dependence of the specific heat of the additional thermal reservoir coupled to electrons (5), i.e. heat capacity normalized by the volume of the absorber,  $C_d/V$ , for three different Cu films. Solid and dashed lines are the phonon and electron specific heats of the films, respectively. (b) Thermal conductance between the reservoir and the electrons (6) per unit volume,  $G_d/V$ . The dashed line shows the electron-phonon thermal conductance  $G_{e-ph}/V$ ; the solid line is the fit of the data for the 50 nm thin film with  $\propto T^4$  dependence.

while for the 50 nm film it roughly follows power-law dependence with the exponent close to 4, which corresponds to  $\alpha = 5$  in Eq. (2).

Our hypothesis about electrically decoupled grains in the film as a reason for the long thermal relaxation time is supported by other experiments. Indeed, previous experiments [31] have demonstrated that thermal relaxation in a uniform silver film follows a single exponential decay with the time constant expected from the theory, while two exponents are needed for a silver film with different grain orientations [22]. Furthermore, the experiments with Cu films evaporated on  $\text{SiO}_2/\text{Si}$  substrate [28, 29] have shown that at the beginning of the growth process a film with  $\langle 111 \rangle$  orientation is formed. Subsequently, grains with  $\langle 110 \rangle$  orientation are nucleated at the boundaries of the  $\langle 111 \rangle$  grains, which results in the growth of  $\langle 110 \rangle$  texture. Afterwards,  $\langle 111 \rangle$  grains can again nucleate at the boundaries between  $\langle 110 \rangle$  grains and so on. In the end, one obtains a sandwiched structure of alternating textures, which might be poorly coupled electrically, especially in our films, which were in contact with atmosphere between fabrication and measurement. It is also well known that electron-phonon scattering rates in bulk Cu are strongly anisotropic [23]. Since in thin films phonon wave vectors are parallel to the surface and since the Fermi velocity of electrons is much higher than the speed of sound, phonons predominantly interact with electrons moving perpendicular to the film surface. Thus, in grains with  $\langle 110 \rangle$  orientation, for example, the scattering rate should be close to that of electrons moving in  $\langle 110 \rangle$  direction in the bulk material. Bulk relaxation time in the  $\langle 110 \rangle$  direction is, indeed, significantly longer than that in  $\langle 111 \rangle$  direction, as magnetic

resonance experiments have shown [23]. In Fig. 3 (b), we plot measured electron-phonon relaxation time in the bulk Cu in  $\langle 110 \rangle$  direction,  $\tau_{\langle 110 \rangle} = 10^{-7} \times (T/1\text{K})^{-3}$  s [23–25], and find that its value is indeed close to measured  $\tau_L$ . Within this scenario, the high value of the pre-factor in front of slowly decaying exponent observed for the 50 nm thin Cu film,  $a \approx 0.8$ , points to the dominant  $\langle 110 \rangle$  texture. For the two 300 nm films  $a$  drops from 0.5 at low  $T$  to 0 at higher  $T$  [22], which hints to  $\langle 111 \rangle$  as preferred orientation.

Though the above arguments qualitatively explain our findings, further experiments and more detailed theoretical modeling are required in order to fully understand heat relaxation mechanisms in thin Cu films. For example, thermal relaxation in the annealed 50 nm film can only be fitted with three exponents and, therefore, cannot be described by the simple model (2). On the other hand, the pronounced effect of annealing on thermal relaxation points at the importance of the grain structure of the film. Yet another unclear issue is the nature of the thermal coupling between conducting and electrically decoupled grains, which is described by the thermal conductance  $G_d$ . We expect such coupling to occur through tunnel barriers between the grains, which would result in  $G_d \propto T$  temperature dependence, but the observed  $G_d \propto T^4$  scaling differs from that. We have also considered an alternative thermal model, in which the additional reservoir couples to film phonons instead of electrons. However, this model results in much smaller values of the pre-factor  $a$  than the observed ones.

In summary, we have investigated dynamic thermal relaxation in Cu films at sub-kelvin temperatures. In contrast to uniform Ag thin films, which are well described by the free electron model [31, 32], thermal relaxation in granular Cu and Ag films shows more complicated behavior with two or even more relaxation times. We explain this phenomenon by the existence of an additional thermal reservoir, which consists of the grains weakly electrically coupled to the current-carrying electrons. Our experiment refines the understanding of non-equilibrium thermal transport in mesoscopic metallic structures and it will help to further optimize the performance of the devices utilizing thermal effects and operating at low temperatures.

We thank O.-P. Saira for technical help, as well as K. L. Viisanen and C. Enss for useful discussions. We acknowledge the provision of the fabrication facilities by Otaniemi research infrastructure for Micro and nanotechnologies (OtaNano). This work was performed as part of the Academy of Finland Centre of Excellence program (Projects No.312057.) and European Research Council (ERC) under the European Union’s Horizon 2020 research and innovation program. (No. 742559 SQH).

---

\* libin.wang@aalto.fi

- [1] F. Giazotto, T. T. Heikkilä, A. Luukanen, A. M. Savin, and J. P. Pekola, *Reviews of Modern Physics* **78**, 217 (2006).
- [2] K. Schwab, E. A. Henriksen, J. M. Worlock, and M. L. Roukes, *Nature* **404**, 974 (2000).
- [3] O. Chiatti, J. T. Nicholls, Y. Y. Proskuryakov, N. Lumpkin, I. Farrer, and D. A. Ritchie, *Physical Review Letters* **97**, 056601 (2006).
- [4] S. Jezouin, F. D. Parmentier, A. Anthore, U. Gennser, A. Cavanna, Y. Jin, and F. Pierre, *Science (New York, N.Y.)* **342**, 601 (2013).
- [5] N. Mosso, U. Drechsler, F. Menges, P. Nirmalraj, S. Karg, H. Riel, and B. Gotsmann, *Nature Nanotechnology* **12**, 430 (2017).
- [6] M. Banerjee, M. Heiblum, A. Rosenblatt, Y. Oreg, D. E. Feldman, A. Stern, and V. Umansky, *Nature* **545**, 75 (2017).
- [7] K. Irwin and G. Hilton, In: Enss C. (eds) *Cryogenic Particle Detection. Topics in Applied Physics*, Springer, Berlin, Heidelberg **99**, 63 (2005).
- [8] B. S. Karasik, A. V. Sergeev, and D. E. Prober, *IEEE Transactions on Terahertz Science and Technology* **1**, 97 (2011).
- [9] L. Miaja-Avila, G. C. O'Neil, Y. I. Joe, B. K. Alpert, N. H. Damrauer, W. B. Doriese, S. M. Fatur, J. W. Fowler, G. C. Hilton, R. Jimenez, C. D. Reintsema, D. R. Schmidt, K. L. Silverman, D. S. Swetz, H. Tatsuno, and J. N. Ullom, *Physical Review X* **6**, 031047 (2016).
- [10] K. M. Morgan, *Physics Today* **71**, 28 (2018).
- [11] M. Nahum and J. M. Martinis, *Applied Physics Letters* **63**, 3075 (1993).
- [12] L. Kuzmin, D. Chouvaev, M. Tarasov, P. Sundquist, M. Willander, and T. Claeson, *IEEE Transactions on Applied Superconductivity* **9**, 3186 (1999).
- [13] J. Govenius, R. Lake, K. Tan, and M. Möttönen, *Physical Review Letters* **117**, 030802 (2016).
- [14] F. C. Wellstood, C. Urbina, and J. Clarke, *Physical Review B* **49**, 5942 (1994).
- [15] Charles Kittel, *Journal of the Mechanics and Physics of Solids* **6**, 83 (2002).
- [16] M. L. Roukes, M. R. Freeman, R. S. Germain, R. C. Richardson, and M. B. Ketchen, *Physical Review Letters* **55**, 422 (1985).
- [17] S. Gasparinetti, K. Viisanen, O.-P. Saira, T. Faivre, M. Arzeo, M. Meschke, and J. Pekola, *Physical Review Applied* **3**, 014007 (2015).
- [18] D. R. Schmidt, C. S. Yung, and A. N. Cleland, *Applied Physics Letters* **83**, 1002 (2003).
- [19] L. B. Wang, O.-P. Saira, and J. P. Pekola, *Applied Physics Letters* **112**, 013105 (2018).
- [20] M. Zgirski, M. Foltyn, A. Savin, K. Norowski, M. Meschke, and J. Pekola, *Physical Review Applied* **10**, 044068 (2018).
- [21] B. Karimi and J. P. Pekola, *Physical Review Applied* **10**, 054048 (2018).
- [22] See Supplementary Material.
- [23] R. E. Doezema and J. F. Koch, *Physical Review B* **6**, 2071 (1972).
- [24] J. F. Koch and R. E. Doezema, *Physical Review Letters* **24**, 507 (1970).
- [25] V. F. Gantmakher and V. A. Gasparov, *Zh. Eksp. Teor. Fiz.* **64**, 1712 (1973).
- [26] V. A. Gasparov, *Zh. Eksp. Teor. Fiz.* **68**, 2259 (1975).
- [27] P. B. Johnson and R. G. Goodrich, *Physical Review B* **14**, 3286 (1976).
- [28] H. L. Wei, H. Huang, C. H. Woo, R. K. Zheng, G. H. Wen, and X. X. Zhang, *Applied Physics Letters* **80**, 2290 (2002).
- [29] H. Huang, H. L. Wei, C. H. Woo, and X. X. Zhang, *Applied Physics Letters* **82**, 4265 (2003).
- [30] L. B. Wang, O.-P. Saira, D. S. Golubev, and J. P. Pekola, *Physical Review Applied* **12**, 024051 (2019).
- [31] K. L. Viisanen and J. P. Pekola, *Physical Review B* **97**, 115422 (2018).
- [32] E. Pinsolle, A. Rousseau, C. Lupien, and B. Reulet, *Physical Review Letters* **116**, 236601 (2016).